Molecular Biology of the Cell
Vol. 17, 163–177, January 2006

Interactions between EHD Proteins and Rab11-FIP2: A Role for EHD3 in Early Endosomal Transport[D]

Naava Naslavsky,* Juliati Rahajeng,* Mahak Sharma, Marko Jović, and Steve Caplan

Department of Biochemistry and Molecular Biology and Eppley Cancer Center, University of Nebraska Medical Center, Omaha, NE 68198-5870

Submitted May 31, 2005; Revised October 7, 2005; Accepted October 14, 2005
Monitoring Editor: Jean Gruenberg

Eps15 homology domain (EHD) 1 enables membrane recycling by controlling the exit of internalized molecules from the endocytic recycling compartment (ERC) en route to the plasma membrane, similar to the role described for Rab11. However, no physical or functional connection between Rab11 and EHD-family proteins has been demonstrated yet, and the mode by which they coordinate their regulatory activity remains unknown. Here, we demonstrate that EHD1 and EHD3 (the closest EHD1 paralog), bind to the Rab11-effector Rab11-FIP2 via EH–NPF interactions. The EHD/Rab11-FIP2 associations are affected by the ability of the EHD proteins to bind nucleotides, and Rab11-FIP2 is recruited to EHD-containing membranes. These results are consistent with a coordinated role for EHD1 and Rab11-FIP2 in regulating exit from the ERC. However, because no function has been attributed to EHD3, the significance of its interaction with Rab11-FIP2 remained unclear. Surprisingly, loss of EHD3 expression prevented the delivery of internalized transferrin and early endosomal proteins to the ERC, an effect differing from that described upon EHD1 knockdown. Moreover, the subcellular localization of Rab11-FIP2 and endogenous Rab11 were altered upon EHD3 knockdown, with both proteins absent from the ERC and retained in the cell periphery. The results presented herein promote a coordinated role for EHD proteins and Rab11-FIP2 in mediating endocytic recycling and provide evidence for the function of EHD3 in early endosome to ERC transport.

INTRODUCTION

Internalization of plasma membrane proteins is a critical event required for multiple physiological cellular processes and its regulation is mediated by a complex web of molecular components (Mellman, 1996; Conner and Schmid, 2003; Benmerah, 2004).

Proteins at the plasma membrane are either internalized into clathrin-coated vesicles (Conner and Schmid, 2003; Benmerah, 2004), or they can be internalized independently of clathrin (Nichols and Lippincott-Schwartz, 2001; Naslavsky *et al*., 2004b). In either case, the internalized vesicles deliver their cargo to the endocytic pathway by fusing with early endosomes (Naslavsky *et al*., 2004b). Although many proteins are transported along the endosomal pathway to late endosomes and lysosomes where they ultimately undergo degradation, some endocytic receptors are returned to the plasma membrane where they continue to exert their physiological effects (Maxfield and McGraw, 2004).

This article was published online ahead of print in *MBC in Press* (http://www.molbiolcell.org/cgi/doi/10.1091/mbc.E05–05–0466) on October 26, 2005.

[D] The online version of this article contains supplemental material at *MBC Online* (http://www.molbiolcell.org).

* These authors contributed equally to this work.

Address correspondence to: Steve Caplan (scaplan@unmc.edu).

Abbreviations used: ERC, endocytic recycling compartment; EHD, Eps15 homology domain; Rab11-FIP2, Rab11-family of interacting proteins 2.

Recycling to the plasma membrane can occur either directly from the early endosome in a process that is not well understood (Sheff *et al*., 1999; Hao and Maxfield, 2000; Sheff *et al*., 2002; van Dam *et al*., 2002) or indirectly through a pericentriolar-localized organelle known as the endocytic recycling compartment (ERC) (Gruenberg and Maxfield, 1995; Maxfield and McGraw, 2004). This compartment is a condensed cellular region containing tubular membrane structures that emanate from the microtubule organizing center (Hopkins and Trowbridge, 1983; Yamashiro *et al*., 1984).

Evidence suggests that endocytic recycling is a complex process whose regulation is attained by a large number of proteins affecting various steps along the endocytic pathway (Prekeris, 2003; Maxfield and McGraw, 2004). Many of these steps are coordinated by Rab-family GTP-binding proteins such as Rab4 and Rab11, whose activity is crucial for transport from early endosomes back to the plasma membrane. Although the role of Rab4 has been described primarily in transport steps initiated at the early endosome (van der Sluijs *et al*., 1992; Daro *et al*., 1996; Sheff *et al*., 1999), Rab11 has been implicated in control of proteins exiting the ERC on route to the plasma membrane (Ullrich *et al*., 1996; Ren *et al*., 1998; Sheff *et al*., 1999; Zeng *et al*., 1999) as well as in sorting events at the early endosome (Sonnichsen *et al*., 2000). Recently, much of the focus on Rab4 and Rab11 activity has concentrated on identifying and characterizing the array of Rab-binding effector proteins involved in the recycling of internalized receptors. The ability of these effectors to link Rab proteins to other proteins is critical for the regulation of Rab-mediated events.

In addition to Rab-family mediated transport and recycling, attention has recently focused on the Eps15 homology domain (EHD)-family of proteins as a part of the complex machinery controlling endocytic recycling (Polo *et al*., 2003; Miliaras and Wendland, 2004) (Supplemental Figure 1A). A genetic screen for *Caenorhabditis elegans* mutants in endocytosis identified the *C. elegans* homologue of EHD1, RME-1, as a component of recycling machinery regulating the return of yolk receptors back to the plasma membrane (Grant *et al*., 2001). Whereas *C. elegans* and *Drospophila melanogaster* express a single C-terminal EHD orthologue, in mammalian cells this family consists of four highly homologous paralogs: EHD1, EHD2, EHD3, and EHD4 (Mintz *et al*., 1999) (Supplemental Figure 1, B and C). All four mammalian EHD proteins are characterized by an N-terminal nucleotide-binding domain, a central coiled-coil region, and a hallmark C-terminal EH domain (Naslavsky and Caplan, 2005) (Supplemental Figure 1A).

Recent studies have demonstrated a role for mammalian EHD1 in the recycling of various receptors back to the plasma membrane (reviewed in Naslavsky and Caplan, 2005). Such receptors include transferrin (Lin *et al*., 2001; Naslavsky *et al*., 2004a), major histocompatibility complex class I (Caplan *et al*., 2002), cystic fibrosis conductance transmitter (Picciano *et al*., 2003), the insulin-responsive glucose transporter (GLUT4) (Guilherme *et al*., 2004b), and α-amino-3-hydroxy-5-methyl-4-isoxazolepropionic acid receptors for long-term potentiation (Park *et al*., 2004a). EHD1 function seems to rely upon its interactions with various NPF-containing proteins, including Rabenosyn-5 (Naslavsky *et al*., 2004a), EHBP1 (Guilherme *et al*., 2004b), and Syndapins (Xu *et al*., 2004; Braun *et al*., 2005). EHD1 may also be involved in several other distinct trafficking steps through the endocytic pathway, including endocytosis of insulin-like growth factor receptor (Rotem-Yehudar *et al*., 2001). One of the major roles of EHD1 seems to be regulating the exit of receptors from the perinuclear ERC back to the plasma membrane. Despite the importance of this family of proteins, much less is known about the other EHD paralogs (EHD2, EHD3, and EHD4) and their putative roles in these pathways. EHD2 links clathrin-mediated endocytosis with the actin cytoskeleton in adipose cells (Guilherme *et al*., 2004a), interacts with GLUT4, and may regulate the recruitment of GLUT4 to the plasma membrane upon exposure to insulin (Park *et al*., 2004b). EHD4 binds to the NPF-containing NUMB protein and functions in regulating endocytic recycling via the small GTP-binding protein Arf6 (Smith *et al*., 2004) and is involved in endocytic transport of nerve growth factor and its receptor (TrkA) in neural cells (Shao *et al*., 2002). EHD3, the protein most closely related to EHD1, oligomerizes with EHD1 and displays a similar subcellular distribution pattern upon overexpression (Galperin *et al*., 2002). However, the precise functional role of EHD3 has not been discerned.

In the current study, we have sought to understand the mechanism by which EHD proteins coordinate endocytic transport and recycling with the Rab11 pathway. We have identified the Rab11 effector protein Rab11-FIP2 as an interaction partner for both EHD1 and EHD3. Our studies support a functional role for EHD3 along the recycling pathway and provide a critical link between EHD-family proteins and the Rab11-mediated recycling pathway.

MATERIALS AND METHODS

Recombinant DNA Constructs

Cloning of Human EHD1 and EHD3 has been described previously (Caplan *et al*., 2002; Naslavsky *et al*., 2004a). EHD3 was subcloned into the EGFP-C3 expression vector after engineering 5′ *Xho*I and 3′ *Eco*RI restriction sites as well as into a pCDNA 3.1(−) vector containing the Myc epitope tag. The EHD1 ΔEH, and G65R mutants lacking the C-terminal EH domain and mutated in the nucleotide binding site, respectively, have been described previously as well as the EH domain (only) of EHD1 (Caplan *et al*., 2002; Naslavsky *et al*., 2004a). The homologous EHD3 ΔEH mutant (generated by introducing a stop codon at amino acid 432) and G65R mutant were generated using the QuikChange site-directed mutagenesis kit (Stratagene, La Jolla, CA). Truncations of EHD1 were generated by introducing stop codons into the GALad-EHD1 constructs at amino acids 432 (EHD1 1–432), 309 (EHD1 1–309), and 199 (EHD1 1–199) using the QuikChange site-directed mutagenesis kit. EHD1 V203P, EHD3 V203P, and EHD3 W485A mutants in GAL4bd vectors as well as in EGFP-C3 and pCDNA 3.1(−) vectors were generated similarly by site-directed mutagenesis. EHD1 EH domain constructs in GAL4bd and Rabenosyn-5 in GAL4ad have been described previously (Naslavsky *et al*., 2004a). Two-hybrid control vectors (GAL4ad-SV40 Large T-antigen and GAL4bd-p53) were obtained from BD Biosciences Clontech (Palo Alto, CA). The long Rab11-FIP2 isoform (GenBank accession no. DQ013303 and Supplemental Figure 2) was cloned by PCR from a human brain library (Marathon-Ready; BD Biosciences Clontech) sequenced and subcloned with 5′ *Eco*RI and 3′ *Bam*HI restriction sites into GAL4ad two-hybrid and EGFP-C3 vectors. Site-directed mutagenesis was used to mutate NPF to APA for each of the three Rab11-FIP2 NPF motifs: GAL4ad-Rab11-FIP2 ΔNPF1 (Rab11-FIP2 with the first NPF motif mutated to APA), GAL4ad-Rab11-FIP2 ΔNPF2 (Rab11-FIP2 with the second NPF motif mutated to APA), and GAL4ad-Rab11-FIP2 ΔNPF3 (Rab11-FIP2 with the third NPF motif mutated to APA). All constructs have been sequence verified and are available upon request. Rip11 and RCP in GAL4bd two-hybrid vectors were generously provided by Dr. R. Prekeris (University of Colorado Health Sciences Center, Denver, CO).

Antibodies

The following antibodies were used in this study: affinity-purified rabbit polyclonal peptide antibodies directed against human EHD1 (DLPPHLVPPSKRRHE) and EHD3 (SQRPIQMVK) and rabbit polyclonal peptide antiserum directed against EHD2 (VERGPDEAMEDGEEGSDDEA) and EHD4 (SHRKSLPKAD) (AnaSpec, San Jose, CA), mouse anti-Myc 9E10 monoclonal antibodies (Covance, Princeton, NJ), rabbit anti-green fluorescent protein (GFP) (Invitrogen, Carlsbad, CA), biotin-conjugated anti-GFP (Rockland, Gilbertsville, PA), rabbit antibodies against Rab11 (US Biologicals, Swampscott, MA), and mouse monoclonals directed against EEA1 and Rab5 (Transduction Laboratories, Newington, NH). Secondary goat anti-mouse 568-nm and donkey anti-rabbit 488-nm antibodies were purchased from Invitrogen. Polyclonal anti-Rab11-FIP2 antibodies were generously provided by Dr. R. Prekeris.

Immunoprecipitations and Immunoblotting

For immunoprecipitation experiments, cells were harvested and lysed for 15 min in buffer containing 25 mM Tris, pH 7.4, 150 mM NaCl, 0.5% Triton X-100 (wt/vol), 0.25 mM 4-(2-aminoethyl)-benzenesulfonyl fluoride, 10 μM leupeptin, 10 μM aprotinin, and 10 mM iodoacetamide. After removal of insoluble matter by centrifugation, the lysate supernatants were subjected to immunoprecipitations with protein A-Sepharose prebound to anti-Myc antibodies. After a 2-h incubation at 4°C, immunoprecipitates were washed four times in lysis buffer containing only 0.1% Triton X-100, and proteins were eluted by boiling in the presence of 1% SDS. Proteins were separated by 10% SDS-PAGE, blocked in 5% nonfat milk in phosphate-buffered saline (PBS), and immunoblotted with biotin-conjugated anti-GFP antibodies. Streptavidin-horseradish peroxidase (HRP) was used to detect the presence of biotinylated anti-GFP antibodies by enhanced chemiluminescence. To immunoprecipitate GFP-tagged proteins, (Supplemental Figure 5), rabbit anti-GFP was used for immunoprecipitating, and immunoblotting was done with mouse anti-Myc (9E10) followed by mouse anti-rabbit light chain HRP (Jackson ImmunoResearch Laboratories, West Grove, PA).

ATP Binding Assay

Cells on 35-mm plates were transfected with the indicated cDNAs, harvested, lysed in 1% Triton X-100 detergent buffer, and cleared lysates were tested for expression by immunoblotting and then incubated with immobilized ATP on polyacrylamide resin according to the manufacturer's instructions (ProteoEnrich ATP binders kit; Novagen-EMD Biosciences, San Diego, CA). Eluted proteins (that were retained on the column) were separated by SDS-PAGE and detected by immunoblotting with anti-Myc or the indicated antibodies directed against endogenous proteins.

Yeast Two-Hybrid Analysis

The *Saccharomyces cerevisiae* strain AH109 (BD Biosciences Clontech) was maintained on YPD agar plates. Transformation was done by the lithium acetate procedure as described in the instructions for the MATCHMAKER two-hybrid kit (BD Biosciences Clontech). For colony growth assays, AH109 cotransformants were streaked on plates lacking leucine and tryptophan and

allowed to grow at 30°C, usually for 3 d, or until colonies were large enough for further assays. An average of three to four colonies was then chosen and suspended in water, equilibrated to the same optical density 600 nm, and replated on plates lacking leucine and tryptophan (+HIS) as well as plates also lacking histidine (−HIS). In addition to regular −HIS plates, some replatings were also done on −HIS plates containing 2 and 10 mM 3-amino-1,2,4-triazole (Fluka, Buchs, Switzerland) to further validate specificity of the interactions.

Gene Knockdown by RNA Interference

RNA interference (RNAi) duplexes (synthesized by Dharmacon, Lafeyette, CO) were transfected using Oligofectamine (Invitrogen) essentially by the method of Elbashir *et al.* (2001) as described for EHD1 (Naslavsky *et al.*, 2004a). Calibration experiments showed that 48 h of treatment was sufficient to attain significantly decreased expression levels of EHD3. The sequence used for EHD1 (base pairs 943–963) was gaaagagatgcccaatgtc, and the sequence for EHD3 (base pairs 579–599) was actggacatctctgatgag.

Immunofluorescence and Transferrin Uptake Assays

HeLa cells were grown on cover glasses, transfected with FuGENE-6 (Roche Diagnostics, Indianapolis, IN), and fixed with 4% (vol/vol) paraformaldehyde in PBS as described previously (Caplan *et al.*, 2001). Fixed cells were incubated with primary antibodies prepared in staining solution [0.2% saponin (wt/vol) and 0.5% (wt/vol) bovine serum albumin (BSA) in PBS] for 1 h at room temperature. After washes in PBS, the cells were incubated with the appropriate fluorochrome-conjugated secondary antibody mixture in staining solution for 30 min at room temperature. Images were acquired using a Zeiss LSM 5 Pascal confocal microscope (Carl Zeiss, Thornwood, NY) by using a 63× 1.4 numerical aperture objective with appropriate filters. Transferrin uptake was studied by first starving the cells in DMEM lacking serum (but containing 0.5% BSA) for 30 min and then applying a 15-min pulse of 1 μg/ml transferrin-Alexa Fluor 568 (Tf-568; Invitrogen). Cells were either fixed and mounted as described above for image analysis or first incubated with the appropriate primary and secondary antibodies before mounting. All images shown are representative images from experiments that have been repeated at least three times.

Quantitative Measurements of Recycling by Flow Cytometry

Cells were serum starved for 30 min and incubated with 1 μg/ml fluorochrome-conjugated transferrin that can be excited at 633 nm (Tf-633; Invitrogen) for a 5-min pulse at 37°C. Cells were then washed three times in PBS, replenished with media containing serum and excess unlabeled holo-transferrin (1 mg/ml), and chased for the indicated times at 37°C [in presence or absence of 100 μM 2-(4-morpholinyl)-8-phenyl-4*H*-1-benzopyran-4-one (LY294002,) a phosphoinositide 3-kinase inhibitor (PI3K), as indicated]. At each time point, cells were washed with PBS, removed from the dish with warm trypsin (15-s treatment), and transferred to precooled tubes containing 10 ml of ice-cold DMEM, and pelleted by centrifugation. Cell pellets were immediately fixed in 300 μl of 4% paraformaldehyde. At least 10,000 cells were analyzed for internal Tf-633 by flow cytometry analysis (BD Biosciences, San Jose, CA).

RESULTS

EHD3 Interacts with Rab11-FIP2

A growing consensus implicates a role for EHD1 in the recycling of internalized proteins from a pericentriolar ERC to the plasma membrane (Lin *et al.*, 2001; Caplan *et al.*, 2002; Picciano *et al.*, 2003; Guilherme *et al.*, 2004b; Naslavsky *et al.*, 2004a; Park *et al.*, 2004a; Xu *et al.*, 2004). Rab11 has also been implicated in control of proteins exiting the ERC en route to the plasma membrane (Ullrich *et al.*, 1996; Ren *et al.*, 1998; Sheff *et al.*, 1999; Zeng *et al.*, 1999) as well as in sorting events at the early endosome (Sonnichsen *et al.*, 2000). Despite the similarities in the proposed functions for Rab11 and EHD1, an interaction or functional link between Rab11 and EHD-family proteins has not been reported, and the mode by which EHD proteins and Rab11 coordinately control recycling remains unknown. Because we found no evidence for a direct interaction between EHD proteins and Rab11 (Supplemental Figure 3), we hypothesized that EHD-family proteins might be linked to Rab11 via one of the growing number of Rab11 effectors. Analysis of the known Rab11 effectors yielded information that only one effector, Rab11-FIP2, contains NPF motifs (three NPF motifs) (Hales *et al.*, 2001; Prekeris *et al.*, 2001; Cullis *et al.*, 2002; Hales *et al.*, 2002; Lindsay and McCaffrey, 2002; Fan *et al.*, 2004; Lindsay and McCaffrey, 2004a), known to interact with proteins containing EH domains (Salcini *et al.*, 1997).

To test whether these proteins interact, we cloned Rab11-FIP2 from a human brain library. The primary PCR product that we identified (Rab11-FIP2 long isoform; deposited to GenBank as accession no. DQ013303) was identical to KIAA0941 (Hales *et al.*, 2001), but it contained an additional insert of 60 base pairs coding for 20 additional amino acids between the second and third NPF motifs, likely because of alternative splicing as predicted by the Berkeley Genome Project Neural Network Splice Site Prediction Program (http://www.fruitfly.org/seq_tools/splice.html; see Supplemental Figure 2 for alignment).

Using yeast two-hybrid binding assays, we tested the binding of EHD1 and EHD3 to Rab11-FIP2 (Figure 1A). Rab11-FIP2 bound to both EHD proteins, which was not surprising because EHD3 is the closest paralog of EHD1 (86.5% identity; see neighbor-joining guide tree in Supplemental Figure 1C). In contrast, no binding of either EHD1 or EHD3 was detected with the Rab11 effectors rip11 and RCP (Supplemental Figure 3). We then tested whether the interactions were indeed mediated via EH-NPF motifs. We have previously demonstrated that a highly conserved tryptophan residue in the EH domain (de Beer *et al.*, 1998, 2000) is essential for the binding of EHD1 to the NPF-containing protein Rabenosyn-5 (Naslavsky *et al.*, 2004a). Accordingly, we generated mutants with a mutation in the same conserved tryptophan residue within the EH domains of EHD3 (EHD3 W485A) and tested the binding of both mutants with Rab11-FIP2. As shown (Figure 1A), binding of EHD1 W485A and EHD3 W485A to either Rabenosyn-5 or Rab11-FIP2 was abrogated, demonstrating that the interaction with Rab11-FIP2 is indeed mediated specifically via the EH domains.

To delineate which of the three Rab11-FIP2 NPF motifs is important for the interactions with EHD1 and EHD3, we used site-directed mutagenesis to mutate each of the three NPF motifs to APA (leaving the proline intact). As demonstrated (Figure 1B), loss of the second NPF motif seemed to be critical for interaction with EHD1 and EHD3, whereas loss of the third NPF motif had little or no effect. Mutating the first NPF motif had a partial effect on the interaction, slowing down the growth of the yeast somewhat. These data suggest that the second NPF motif plays a key role in binding to the EH domain of EHD1 and EHD3 and that the other two NPF motifs might either strengthen the interactions or mediate additional interactions with EH domain-containing proteins.

To verify the significance of these interactions in vivo, we sought to coimmunoprecipitate EHD proteins and Rab11-FIP2 from cell lysates. To this aim, we cotransfected cells with GFP-Rab11-FIP2 and either Myc-EHD3 or Myc-EHD1 (Figure 1C, lanes 2 and 4, respectively). Control experiments were done by cotransfecting Myc-EHD3 ΔEH or Myc-EHD1 ΔEH together with GFP-Rab11-FIP2 (Figure 1C, lanes 3 and 5, respectively). Additional controls included the use of GFP with Myc-EHD3 (Figure 1C, lane 1) and GFP-Rab11-FIP2 with MycVam6p (a lysosomal protein) (Figure 1C, lane 6). All cotransfections were effective (Figure 1C, center and bottom), and bands corresponding to GFP-Rab11-FIP2 and Myc-tagged EHD proteins could be readily detected. As we predicted on the basis of the two-hybrid binding studies, both wild-type EHD proteins immunoprecipitated Rab11-FIP2 (Figure 1C, top, lanes 2 and 4), whereas ΔEH truncations induced a complete loss of binding (Figure 1C, top,

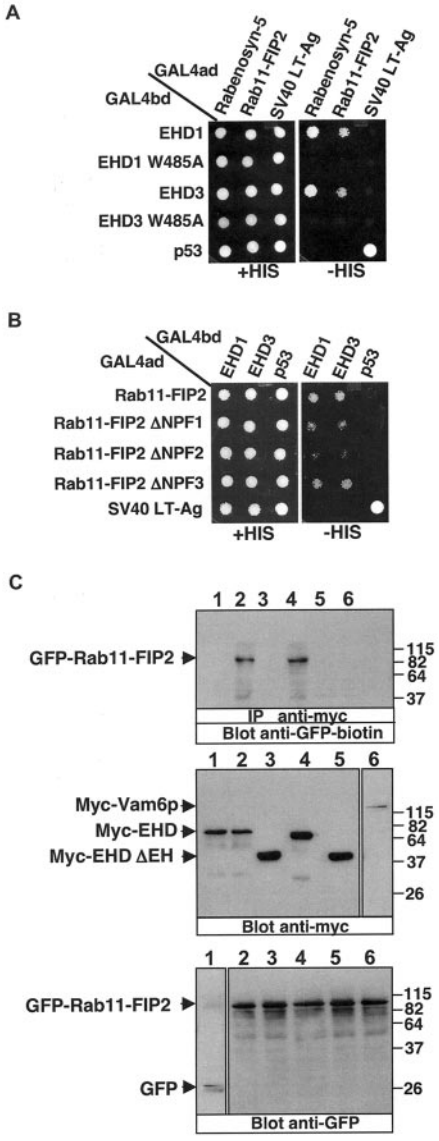

Figure 1. Interaction between EHD proteins and Rab11-FIP2. (A and B) The *S. cerevisae* yeast strain AH109 was cotransformed with the following GAL4 binding domain (GAL4bd) fusion constructs: GAL4bd-EHD1, GAL4bd-EHD1 W485A, GAL4bd-EHD3, GAL4bd-EHD3 W485A, and GAL4bd-p53 (control) together with the following GAL4 transcription activation (GAL4ad) fusion products: GAL4ad-Rabenosyn-5, GAL4ad-Rab11-FIP2, GAL4ad-Rab11-FIP2 ΔNPF1, GAL4ad-Rab11-FIP2 ΔNPF2, GAL4ad-Rab11-FIP2 ΔNPF3, and GAL4ad-SV40 Large T-antigen (control). Cotransformants were assayed for their growth on nonselective (+HIS) and selective (−HIS) media. (C) HeLa cells were cotransfected with either GFP and Myc-EHD3 (lane 1), GFP-Rab11-FIP2 and Myc-EHD3 (lane 2), GFP-Rab11-FIP2 and Myc-EHD3 ΔEH (lane 3), GFP-Rab11-FIP2 and Myc-EHD1 (lane 4), GFP-Rab11-FIP2 and Myc-EHD1 ΔEH (lane 5), or GFP-Rab11-FIP2 and Myc-Vam6p (lane 6). After 24 h, cells were harvested, lysed, and subjected to immunoprecipitations with antibodies against the Myc-epitope. Immunoprecipitates (top) and total lysates (center and bottom) were resolved by 10% SDS-PAGE, transferred to nitrocellulose, and immunoblotted with biotinylated anti-GFP followed by streptavidin-HRP (top), the Myc-epitope followed by anti-mouse-HRP conjugated antibodies (center), or with anti-GFP antibodies followed by anti-rabbit-HRP (bottom). Enhanced chemiluminescence was used for detection. Different film exposure times were obtained for Myc-Vam6p (center, lane 6) and GFP (bottom, lane 1).

lanes 3 and 5). These data demonstrate that EHD1 and EHD3 interact with Rab11-FIP2 in vivo in an EH-dependent manner.

EHD Proteins Regulate the Localization of Rab11-FIP2

To begin addressing the functional significance of the interactions between EHD proteins and a component of the Rab11 recycling pathway, we expressed the GFP-tagged Rab11-FIP2. As described previously (Hales *et al*., 2001; Cullis *et al*., 2002; Hales *et al*., 2002; Lindsay and McCaffrey, 2002; Fan *et al*., 2004), Rab11-FIP2 localized to peripheral endocytic vesicles, but it had a concentration of vesicles at the perinuclear region of the cell (Figure 2A). In addition to the vesicular structures, putative tubular endosomes could occasionally be observed, although they were fewer than those observed in cells expressing Myc-EHD3 (Figure 2B) or Myc-EHD1 (Caplan *et al*., 2002). To assess whether the interactions between C-terminal EHD proteins and Rab11-FIP2 had any observable functional consequences in vivo, we coexpressed the wild-type proteins in HeLa cells (Figure 2, D–F). Wild-type EHD3 exhibited its typical tubulovesicular pattern (Figure 2E), resembling its distribution when expressed alone (Figure 2B). However, the coexpression of transgenic EHD3 together with GFP-Rab11-FIP2 had a dramatic effect on the subcellular localization of Rab11-FIP2; rather than being primarily on vesicular structures, it now localized primarily to tubular structures that aligned and colocalized with those of EHD3 (Figure 2D). Myc-EHD3 overexpression also induced the recruitment of endogenous Rab11-FIP2 to tubular membrane structures, although the effect was not as striking as that observed upon transfecting GFP-Rab11-FIP2 (Supplemental Figure 4, A–C). Overexpression of EHD3 had no observable effect on other endosomal proteins (transfected or endogenous), such as EEA1 and Rab5 (our unpublished observations). EHD1 had a similar effect on Rab11-FIP2 to that observed with EHD3 (Supplemental Figure 4, D–F). We hypothesized that the effect of EHD proteins on Rab11-FIP2 was mediated via interactions between the EH domains of EHD3 and EHD1 with the Rab11-FIP2 NPF motifs. We have previously demonstrated that truncation of the EHD1 EH domain induces this mutant to lose its tubular pattern and localize primarily to vesicular endosomal structures (Caplan *et al*., 2002). We therefore generated an EHD3 ΔEH mutant, and not surprisingly, when expressed alone EHD3 ΔEH displayed a punctate vesicular pattern (Figure 2C) similar to that of EHD1 ΔEH (Caplan *et al*., 2002). To determine whether the EHD3 EH domain was required for the recruitment of Rab11-FIP2 to tubulovesicular membranes, we coexpressed GFP-Rab11-FIP2 together with Myc-EHD3 ΔEH (Figure 2, G–I). Consistent with a role for EH-NPF interactions in mediating the recruitment of Rab11-FIP2, the localization of Rab11-FIP2 was not altered by EHD3 ΔEH, and although both proteins maintained their vesicular distribution patterns observed when transfected individually and localized to vesicular structures with a concentration at the ERC (Figure 2, A and C), overall the level of colocalization remained low (Figure 2, G–I). These data suggest that EHD proteins recruit Rab11-FIP2 to endosomal membranes.

EHD Nucleotide Binding Affects Its Membrane Association and Regulates the Localization of Rab11-FIP2

It has been demonstrated that the nucleotide binding site of EHD1 plays a critical role in its function and that mutants blocking nucleotide binding (EHD1 G65R) show impaired recycling (Grant *et al*., 2001; Lin *et al*., 2001; Caplan *et al*.,

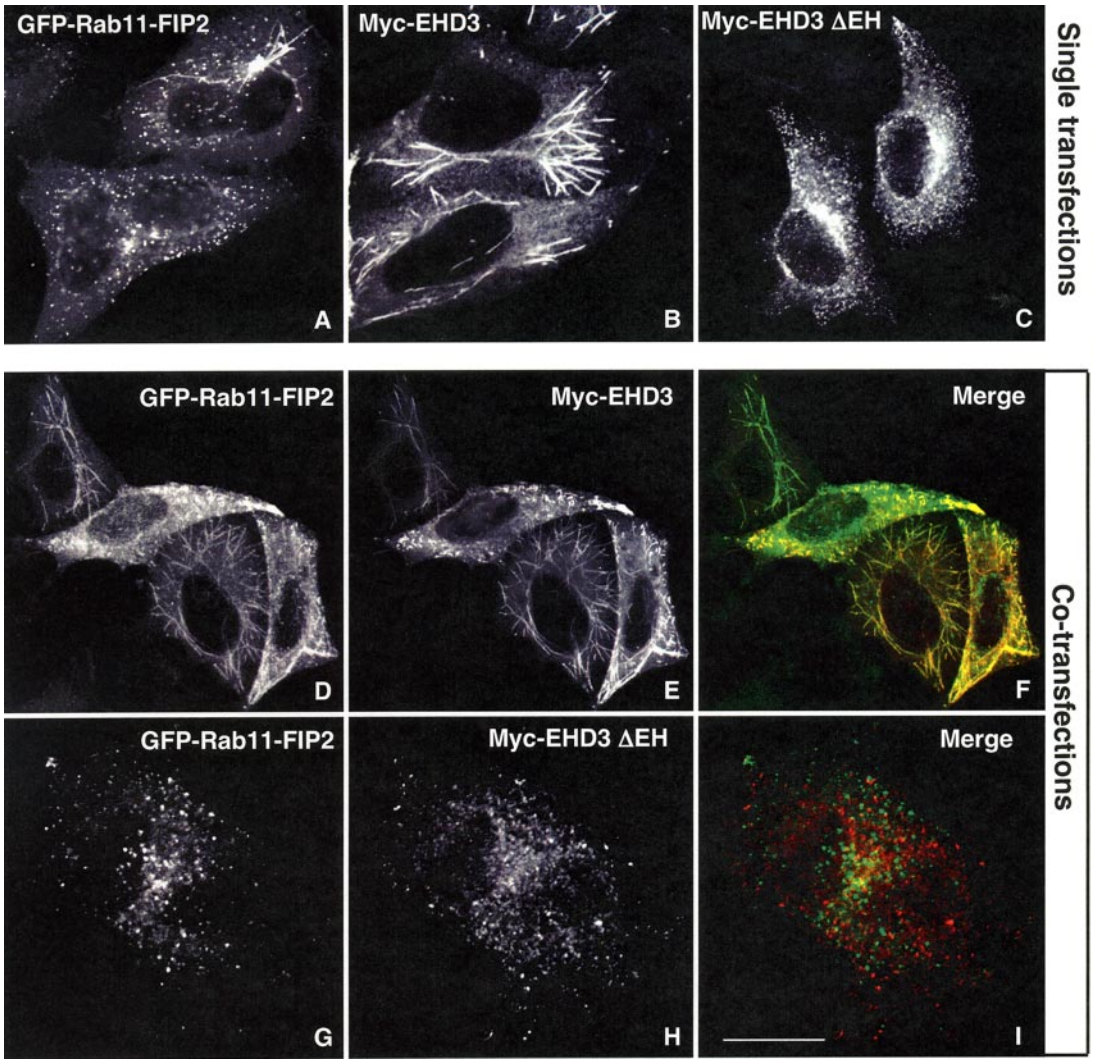

Figure 2. Recruitment of Rab11-FIP2 to EHD-containing membranes. (A–I) HeLa cells on coverglasses were transfected with GFP-Rab11-FIP2 (A), Myc-EHD3 (B), Myc-EHD3 ΔEH (C), or cotransfected with either GFP-Rab11-FIP2 and Myc-EHD3 (D–F), or with GFP-Rab11-FIP2 and Myc-EHD3 ΔEH (G–I). After 24 h, cells were fixed (A) or incubated with mouse monoclonal antibody to the Myc epitope (B–I). After washing, cells were incubated with 568-conjugated goat anti-mouse antibody (red channel) and mounted on coverslides. All images were obtained using a Zeiss LSM 5 Pascal confocal microscope. Bar, 10 μm.

2002; Picciano *et al*., 2003; Park *et al*., 2004a). We hypothesized that mutations in the nucleotide-binding sites of EHD1 and EHD3 might affect binding to NPF-containing proteins. It has been shown recently that EHD1 binds ATP (Lee *et al*., 2005), but the nucleotide binding capability of EHD3 has not been confirmed. To investigate this, we transfected cells with Myc-EHD1, Myc-EHD1 G65R (deficient in nucleotide binding), Myc-EHD3, or Myc-EHD3 G65R (putative deficiency in nucleotide binding) (Figure 3A). Cell lysates were tested for expression (Figure 3A, bottom), and lysates were incubated with an immobilized ATP on polyacrylamide resin. Binding of the transfected Myc-tagged proteins to the ATP-resin was detected by immunoblot analysis (Figure 3A, top). As shown, both EHD1 and EHD3 bound to the ATP resin. However, the G65R mutants showed little or no binding, suggesting that ATP binding by EHD proteins was achieved by a similar mechanism, dependent upon glycine 65 and the surrounding motif. As a control, the eluates were blotted with actin, which is an ATP-binding protein (Jacobson and Rosenbusch, 1976; Kinosian *et al*., 1993), and with Rab4, which binds GTP but not ATP (Figure 3A, bottom and middle, respectively).

Having demonstrated that EHD3 binds ATP, we then used two-hybrid analysis to test whether nucleotide binding is necessary for EHD proteins to interact with the NPF-containing proteins Rabenosyn-5 and Rab11-FIP2 (Figure 3B). As shown, both EHD1 G65R and EHD3 G65R were capable of binding to Rabenosyn-5 and Rab11-FIP2, but the loss of ATP-binding partly reduced the efficiency of these interactions compared with the wild-type EHD proteins (Figure 3B).

To test the effect of the impaired nucleotide-binding EHD1 and EHD3 mutants in vivo on the localization of Rab11-FIP2, we coexpressed Myc-EHD3 G65R with GFP-Rab11-FIP2 (Figure 3, D and E) or Myc-EHD1 G65R with GFP-Rab11-FIP2 (Figure 3, F and G). When expressed alone, GFP-Rab11-FIP2 distributed in a typical vesicular pattern with a concentration of tubules emanating from the ERC region (Figure 3C). As we predicted, the EHD3 G65R mutant (Figure 3E) behaved similarly to EHD1 G65R (Figure 3G), be-

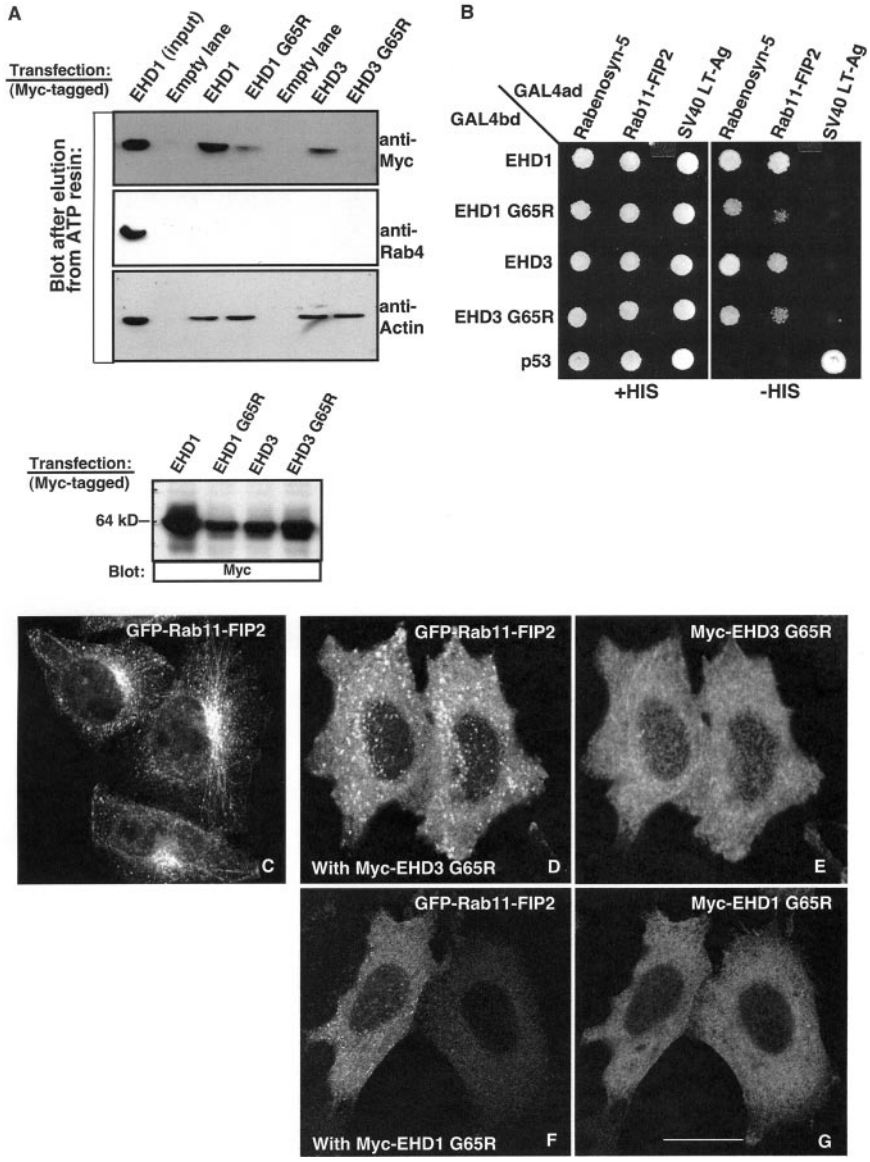

Figure 3. EHD3 binds ATP and nucleotide binding regulates Rab11-FIP2 association and localization. (A) HeLa cells were transfected with either Myc-EHD1, Myc-EHD1 G65R, Myc-EHD3, or Myc-EHD3 G65R. Expression levels of the transgenes were monitored with anti-Myc antibody by immunoblot analysis (bottom). One volume of Myc-EHD1 G65R, Myc-EHD3, and Myc-EHD3 G65R lysates, and one-third volume of the Myc-EHD1 lysate (due to higher expression levels of this cDNA) were subjected to binding on an immobilized ATP polyacrylamide resin. Proteins were eluted from the resin, separated by SDS-PAGE, and binding of transgenic proteins was detected with anti-Myc antibodies and immunoblot analysis (top). The left lane shows 5% of the "input" lysate (not subjected to the ATP resin). As controls, the input sample and eluates were also subjected to immunoblot analysis with anti-Rab4 (second panel; non-ATP binding protein) and anti-actin (third panel; ATP-binding protein) (B) The *S. cerevisiae* yeast strain AH109 was cotransformed with the following GAL4 DNA-binding domain (GAL4bd) constructs: GAL4bd-EHD1, GAL4bd-EHD1 G65R, GAL4bd-EHD3, GAL4bd-EHD3 G65R, and GAL4bd-p53 (control) together with the following GAL4 transcription activation fusion products GAL4ad-Rabenosyn-5, GAL4ad-Rab11-FIP2, and GAL4bd-SV40 LT-Ag (control). Cotransformants were assayed for their growth on nonselective (+HIS) and selective (−HIS) media. (C–G) HeLa cells on cover-glasses were transfected with GFP-Rab11-FIP2 (C) or cotransfected with either GFP-Rab11-FIP2 and Myc-EHD3 G65R (D and E) or GFP-Rab11-FIP2 and Myc-EHD1 G65R (F and G). After 24 h, cells were fixed, permeabilized, and incubated with mouse monoclonal antibody to the Myc epitope followed by a 568-conjugated goat anti-mouse antibody before mounting on coverslides (D–G). The GFP-Rab11-FIP2 was fixed and mounted directly (C). All images were obtained using a Zeiss LSM 5 Pascal confocal microscope. Bar, 10 μm.

coming mostly cytosolic, and losing its typical tubulovesicular pattern (Lin *et al*., 2001; Caplan *et al*., 2002). The effect of either EHD mutant on the localization of Rab11-FIP2 was dramatic, and the latter protein also became mostly cytosolic, with some punctate vesicles still visible (Figure 3, D and F). These results suggest that EHD nucleotide binding can regulate the localization of Rab11-FIP2.

Hetero-Oligomerization Is Controlled by EHD Nucleotide Binding

A recent study showed that the EHD1 G65R mutant, impaired in its ability to bind nucleotides, loses its ability to form homodimers (Lee *et al*., 2005). EHD1 and EHD3 form hetero-oligomeric complexes in vivo (Galperin *et al*., 2002; Supplemental Figure 5), and we have previously shown that endogenous EHD proteins migrate in large complexes when subjected to sedimentation velocity analysis (Caplan *et al*., 2002). Therefore, we reasoned that hetero-oligomerization may also be regulated by EHD nucleotide-binding status. For EHD1/EHD3 hetero-oligomerization to have physiological significance, we first checked whether both endogenous proteins are expressed in the same cells. Determining whether endogenous EHD1 and EHD3 proteins are coexpressed has been complicated by the high degree of identity between them, particularly in regions predicted to be immunogenic. We generated rabbit polyclonal peptide antibodies against highly specific amino acids stretches in the four EHD paralogs (Supplemental Figure 1B, orange underlined regions), and these antibodies were capable of specifically detecting each of the four proteins by immunoblotting analysis with no detectable cross-reactivity. As indicated, all four endogenous proteins are expressed in human HeLa cells (Figure 4A) as well as in normal mouse fibroblasts (our unpublished observations).

Having shown that both endogenous EHD1 and EHD3 are expressed in the same cells, we now turned to determine whether hetero-oligomerization is affected by the nucleotide status of EHD1 and EHD3. By two-hybrid analysis (Figure 4B), we showed that although wild-type EHD1 and EHD3 proteins bind to themselves and each other, the loss of nucleotide-binding impairs both homo-oligomerization (consistent with the report of Lee *et al*., 2005) and hetero-

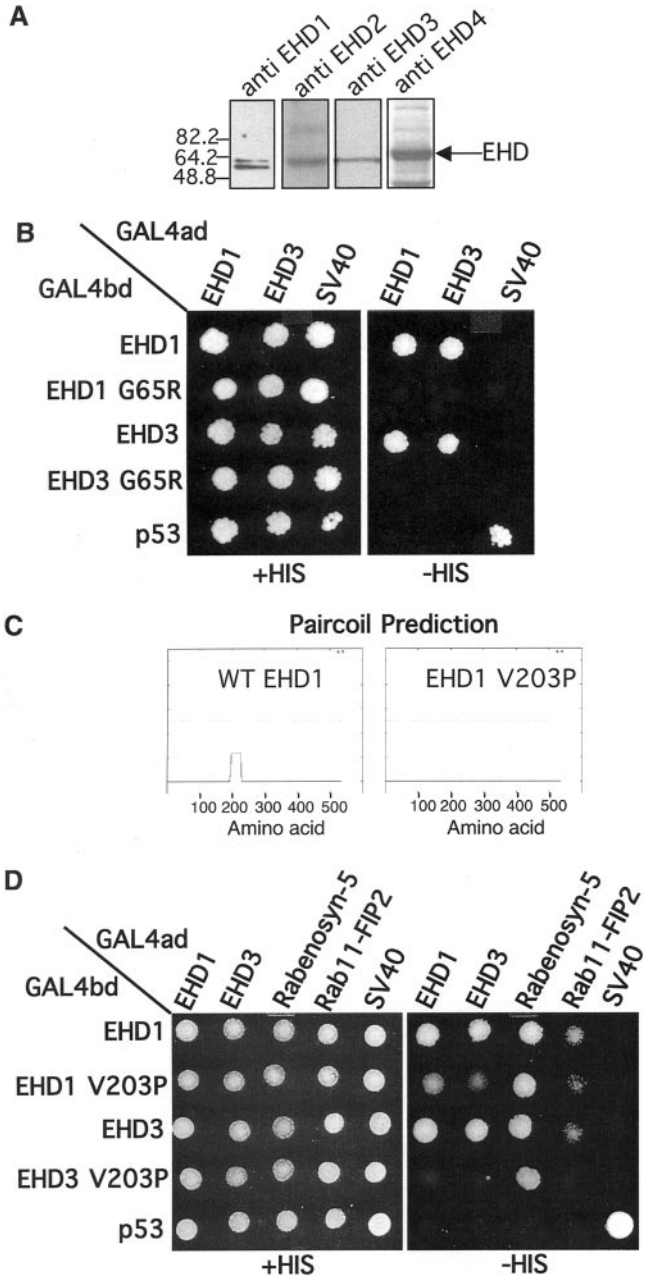

Figure 4. Delineation of the EHD protein requirements for oligomerization. (A) Proteins from HeLa cell lysates were separated by 10% SDS-PAGE, transferred to nitrocellulose filters, and immunoblotted with polyclonal peptide antibodies specific for human EHD1, EHD2, EHD3, and EHD4. EHD1 and EHD3 antibodies were affinity purified on a column containing the specific peptides. Crude antiserum was used to detect EHD2 and EHD4. The arrow denotes the ~60-kDa EHD proteins. (B–D) The *S. cerevisae* yeast strain AH109 was cotransformed with the following GAL4 DNA-binding domain (GAL4bd) fusion products: GAL4bd-EHD1, GAL4bd-EHD1 G65R, GAL4bd-EHD3, GAL4bd-EHD3 G65R, GAL4bd-EHD1 V203P, GAL4bd-EHD3 V203P, and GAL4bd-p53 (control) together with the following GAL4 transcription activation fusion constructs (GAL4ad): GAL4ad-EHD1, GAL4ad-EHD3, GAL4ad-Rabenosyn-5, GAL4ad-Rab11-FIP2, and GAL4ad-SV40 Large T Antigen (control). Cotransformants were assayed for their growth on nonselective (+HIS) and selective (−HIS) media. Paircoil predictions depicted in C were done at the following site: http://paircoil.lcs.mit.edu/cgi-bin/paircoil.

oligomerization (Figure 4B). These data suggest that hetero-oligomerization between EHD1 and EHD3 likely occurs in cells and that this depends upon the ability of each protein to bind nucleotides.

Oligomerization Is Necessary for Interactions between EHD Proteins and Rab11-FIP2

To test whether oligomerization might also be a prerequisite for the EHD/Rab11-FIP2 associations, we first aimed to identify EHD1 and EHD3 point mutants incapable of hetero-oligomerizing. Because it has been determined recently that the coiled-coil region of EHD1 is needed for homo-oligomerization (Lee *et al*., 2005), we sought to determine whether EHD1/EHD3 hetero-oligomerization is similarly mediated, and if so, to further delineate the oligomerization site (Figure 4, C and D). To identify the specific binding regions between EHD1 and EHD3, we first analyzed a series of deletion/truncation mutants in their ability to bind to each other by two-hybrid analysis and found that the central coiled-coil region is indeed critical for binding (Supplemental Figure 6). To identify a more specific region necessary for oligomerization, we used the Paircoil prediction program (http://paircoil.lcs.mit.edu/cgi-bin/paircoil) and identified a sequence from about amino acid 193 on to 227 with the greatest propensity to form a coiled-coil (Figure 4C). Within this region, we identified a conserved valine residue at amino acid 203 predicted to be critical for formation of coiled-coils within EHD1 and EHD3. Accordingly, we then generated V203P mutants for both EHD1 and EHD3 and tested their ability to oligomerize and interact with Rabenosyn-5 and Rab11-FIP2 (Figure 4D). As demonstrated, wild-type EHD1 and EHD3 proteins oligomerized and associated with Rabenosyn-5 and Rab11-FIP2 but not with the negative control protein p53. However, the coiled-coil mutant EHD1 V203P displayed greatly reduced binding to EHD3 and weak homo-oligomerization. EHD3 V203P exhibited a similar pattern, showing little or no homo- and hetero-oligomerization. In contrast, binding of both EHD1 V203P and EHD3 V203P to Rabenosyn-5 via their EH domains remained intact. However, the interactions between EHD proteins and Rab11-FIP2 were inhibited by the V203P mutations, suggesting that oligomerization is a requirement for EH-mediated binding to Rab11-FIP2 but not Rabenosyn-5.

A Role for EHD3 in Mediating Transport from the Early Endosome

The oligomerization of EHD1 and EHD3, together with the binding of these proteins to Rab11-FIP2, led us to hypothesize a related role for these interactors in orchestrating endocytic recycling events. Although EHD1 and Rab11-FIP2 have been implicated in recycling, the function of EHD3 has not been determined. To address the function of EHD3, we used RNAi to reduce its cellular expression levels. HeLa cells were treated with Mock-RNAi, or RNAi specific for either EHD1 or EHD3 (Figure 5A). As demonstrated in the top panel, both EHD1- and EHD3-RNAi treatments resulted in a significant decrease in EHD1 and EHD3 protein levels, respectively. Similar loading of samples was confirmed by Coomassie blue staining (our unpublished observations). Despite the considerable homology between EHD1 and EHD3 proteins, RNAi for both EHD1 and EHD3 was highly specific and had little effect on expression levels of the other EHD protein (Figure 5A), further confirming the specificity of the RNAi and EHD antibodies.

We have previously shown that reduced levels of EHD1 expression caused a delay in recycling to the plasma membrane and an accumulation of internalized receptor in the

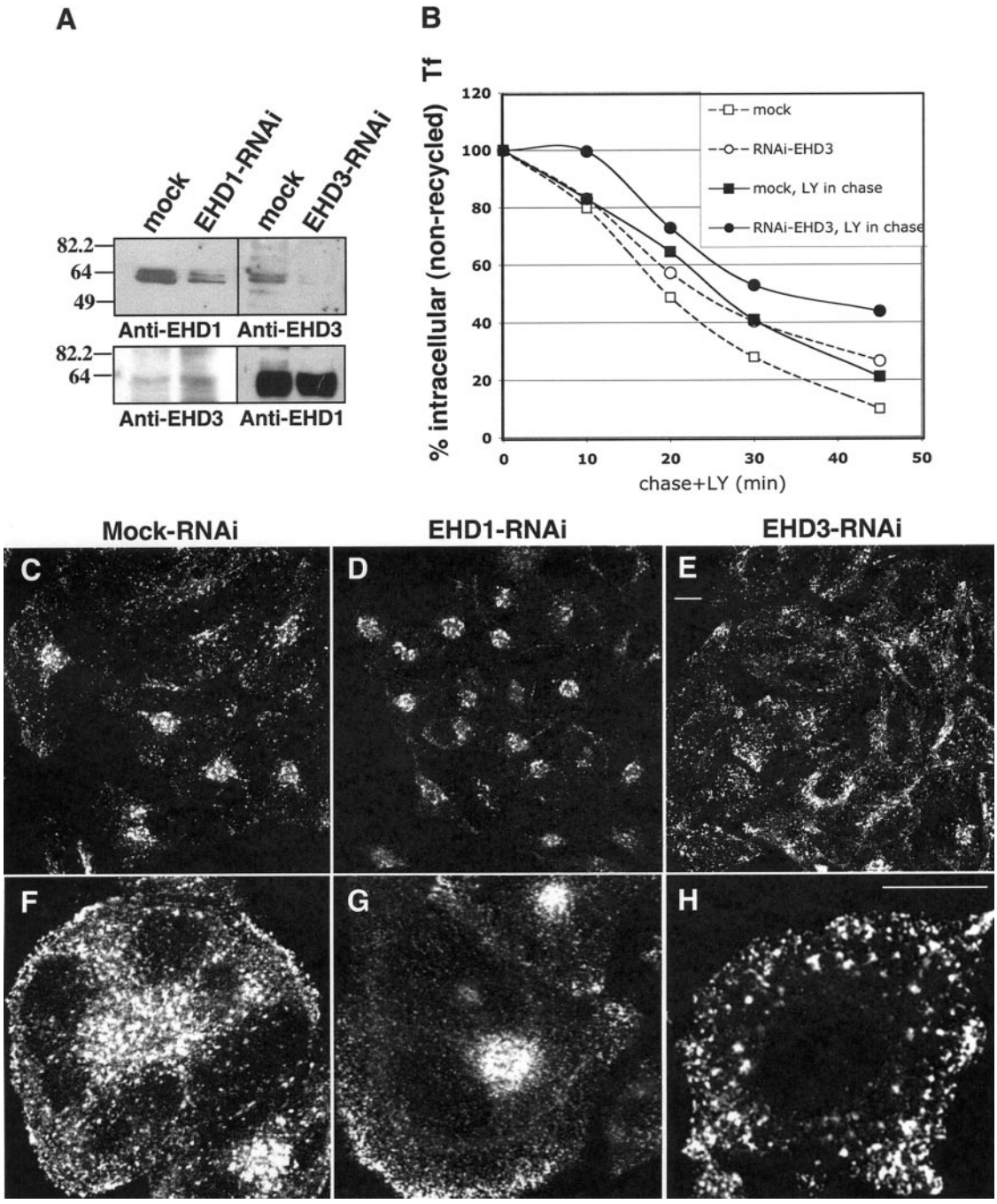

Figure 5. Loss of EHD3 expression inhibits access of internalized transferrin to the endocytic recycling compartment. (A) HeLa cells were treated with either Mock-, EHD1-, or EHD3-RNAi and harvested after 48 h. Cells were lysed and proteins were separated by 10% SDS-PAGE, transferred to nitrocellulose filters, and subjected to immunoblotting with affinity-purified anti-EHD1 antibodies (top left) or purified anti-EHD3 antibodies (top right). The filters were then stripped with 3 M guanidine thiocyanate; Mock- and EHD1-RNAi-treated cells were then incubated reciprocally with anti-EHD3 (bottom left) and anti-EHD1 (bottom right). (B) HeLa cells were Mock-treated (squares) or EHD3-RNAi-treated (circles), serum starved, and then incubated with labeled transferrin (Tf-633) for 5 min at 37°C. After washing and removing unbound Tf-633, the cells were incubated in full media containing excess holo-transferrin and chased for the times indicated, in the presence (black) or absence (unfilled) of 100 μM LY294002 (LY). Cells were harvested by a brief trypsinization, fixed, and analyzed by flow cytometry to determine levels of internal Tf-633. (C–H) HeLa cells on coverglasses treated with Mock-RNAi (C and F), EHD1-RNAi (D and G), or EHD3-RNAi (E and H) for 48 h were pulsed with transferrin-Alexa-Fluor (Tf-568) for 15 min and fixed. Subcellular distribution of internalized Tf-568 was analyzed by confocal microscopy. Bars (C–E and F–H), 10 μm.

ERC (Naslavsky *et al*., 2004a). Accordingly, we tested whether loss of EHD3 expression causes similar alterations in endocytic transport. Mock-treated cells that were pulsed for 15 min with fluorescently labeled transferrin exhibited transferrin in the ERC as well as in peripheral endocytic structures (Figure 5, C and F). As expected, EHD1-RNAi

induced an accumulation of the transferrin in a compact ERC, with little localized to the cell periphery (Figure 5, D and G). Surprisingly, EHD3-RNAi did not cause a similar effect to that seen with EHD1-RNAi; instead, most of the internalized transferrin was observed in somewhat enlarged peripheral structures, with very little transferrin reaching the ERC (Figure 5, E and H). These data are consistent with a role for EHD3 in endocytic events differing from that of EHD1.

To determine whether loss of EHD3 expression impaired the rate of recycling, we compared the kinetics of transferrin recycling by a pulse-chase flow cytometry assay (Figure 5B). Cells with reduced EHD3 expression displayed a small but consistent delay in the recycling of transferrin. The presence of the PI3K inhibitor LY294002 (proposed to interfere with the fast recycling pathway; van Dam *et al*., 2002) slowed the overall rate of recycling (for Mock-treated cells), and further delays were observed in the rate of recycling for cells treated with EHD3-RNAi (Figure 5B).

Because the loss of EHD3 expression causes the accumulation of transferrin in peripheral organelles (Figure 5, E and H), we hypothesized that these structures are early endosomes and that EHD3 may be required for the transport stage between early endosomes and the ERC. To characterize these vesicles, we treated HeLa cells with either Mock- or EHD3-RNAi and allowed the cells to internalize labeled transferrin. The cells were then fixed, permeabilized, and immunostained with antibodies against the endogenous early endosomal markers EEA1 (Figure 6, A–F) and Rab5 (our unpublished observations). As expected, in Mock-treated cells, the internalized transferrin was localized both to the ERC and distributed throughout the periphery (Figure 6B), displaying a high degree of colocalization with EEA1 (Figure 6, A–C) and Rab5 (our unpublished observations). Consistent with Figure 5, the transferrin in cells treated with EHD3-RNAi seemed not to reach the ERC and was observed primarily in the periphery, often in large punctate structures (Figure 6E). It is noteworthy that loss of EHD3 also had an effect on both EEA1 and Rab5, with both early endosomal markers now mostly absent from the perinuclear region, and observed primarily on large peripheral structures that colocalized with internalized transferrin (Figure 6, D–F; our unpublished observations). These data show that in the absence of EHD3, transferrin is indeed retained at peripheral early endosomal structures and not at the ERC. To further confirm the proposed differences in function of EHD1 and EHD3, we used affinity-purified antibodies to characterize the endogenous distribution of EHD3. As we have shown previously, endogenous EHD1 resides primarily in an array of tubulovesicular structures (Figure 6G; Caplan *et al*., 2002). Endogenous EHD3, however, seemed to be primarily localized to punctate vesicular membranes (Figure 6, H and J). Coincubation of the purified EHD3 antibody with the peptide used for immunizations demonstrated the specificity of the staining (Figure 6I). To determine whether endogenous EHD3 is indeed localized to early endosomes, we costained with antibodies for EEA1. As shown, both endogenous EHD3 and EEA1 partially overlapped in the perinuclear region as well as in the periphery on punctate structures (Figure 6, J–L, inset). Similar partial colocalizations were observed with Rab5, another early endosomal marker (our unpublished observations). Together, these results suggest a role for EHD3 in transport from early endosomes to the ERC.

EHD3 Is Required for Recruitment of Rab11-FIP2 to the ERC

Most studies on Rab11 support a role for this small GTPase at the ERC in controlling exit of receptors and their recycling to the plasma membrane (Ullrich *et al*., 1996; Ren *et al*., 1998; Sheff *et al*., 1999; Zeng *et al*., 1999). However, Rab11 also localizes to early/sorting endosomes, where it is segregated to micromembrane domains that differ from those containing Rab4 and Rab5 (Sonnichsen *et al*., 2000). Because our data promotes a role for EHD3 in transport of receptors to the ERC, and given the interaction that we have characterized with the Rab11 effector Rab11-FIP2, we hypothesized that EHD3 may regulate transport of Rab11-FIP2 and Rab11 from early endosomes to the ERC. To test this hypothesis, HeLa cells were treated with either Mock-RNAi, EHD3-RNAi, or EHD1-RNAi, and transfected with GFP-Rab11-FIP2, before being pulsed with labeled-transferrin (Figure 7). In Mock-treated cells, transferrin was observed throughout the cell in a typical endosomal distribution, with an accumulation at the ERC (Figure 7B). Moreover, some of the peripheral transferrin-containing vesicles and many of the ERC-based vesicles seemed to colocalize with GFP-Rab11-FIP2 vesicles (Figure 7, A–C, inset and arrows). However, EHD3-RNAi-treated cells exhibited a lack of transferrin at the ERC and a preponderance of large peripheral structures (Figure 7E), and GFP-Rab11-FIP2 was prevented from localizing to the ERC and was retained in large peripheral structures showing partial costaining with the internalized transferrin (Figure 7, D–F). When the same experiment was done using EHD1-RNAi, the internalized transferrin accumulated, as expected, at the ERC region (Figure 7H). Indeed, the GFP-Rab11-FIP2 also seemed to accumulate in this region (Figure 7, G–I), suggesting that both endogenous EHD proteins affect the subcellular itinerary of Rab11-FIP2, albeit each in a different manner. Endogenous EHD3 also showed a partial colocalization with GFP-Rab11-FIP2 (Figure 7, J–L). We next reasoned that if the loss of EHD proteins affect the localization of Rab11-FIP2, they may similarly have a bearing on the localization of Rab11, because Rab11-FIP2 associates with both GDP- and GTP-bound Rab11 (Hales *et al*., 2001). As expected, in Mock-treated cells, internalized transferrin colocalized extensively with endogenous Rab11, at the ERC and in small peripheral endosomes (Figure 8, A–C). However, in cells treated with EHD3-RNAi, not only was there very little internalized transferrin at the ERC, but the endogenous Rab11 was also absent from the ERC and seemed dispersed in very small vesicles and/or in the cytoplasm (Figure 8, D–F). The effect of EHD1-RNAi on Rab11 was difficult to determine by such experiments, because it has been well established that Rab11 displays a concentrated distribution at the ERC (Lapierre *et al*., 2003). Overall, these data are consistent with a role for EHD proteins in regulating Rab11-FIP2 transport and possibly linking EHD-family proteins to the Rab11-mediated recycling pathway.

DISCUSSION

The question of whether EHD proteins and Rab11 regulate distinct recycling pathways or whether they coordinate recycling events through a common pathway is critical to our understanding of the mechanisms controlling endocytic recycling. Despite concerted attempts, we have been unsuccessful in identifying a direct link between Rab11 and EHD-family proteins. Much effort has recently focused on studying newly identified Rab11 effectors proteins, and we reasoned that EHD-family proteins might be connected in-

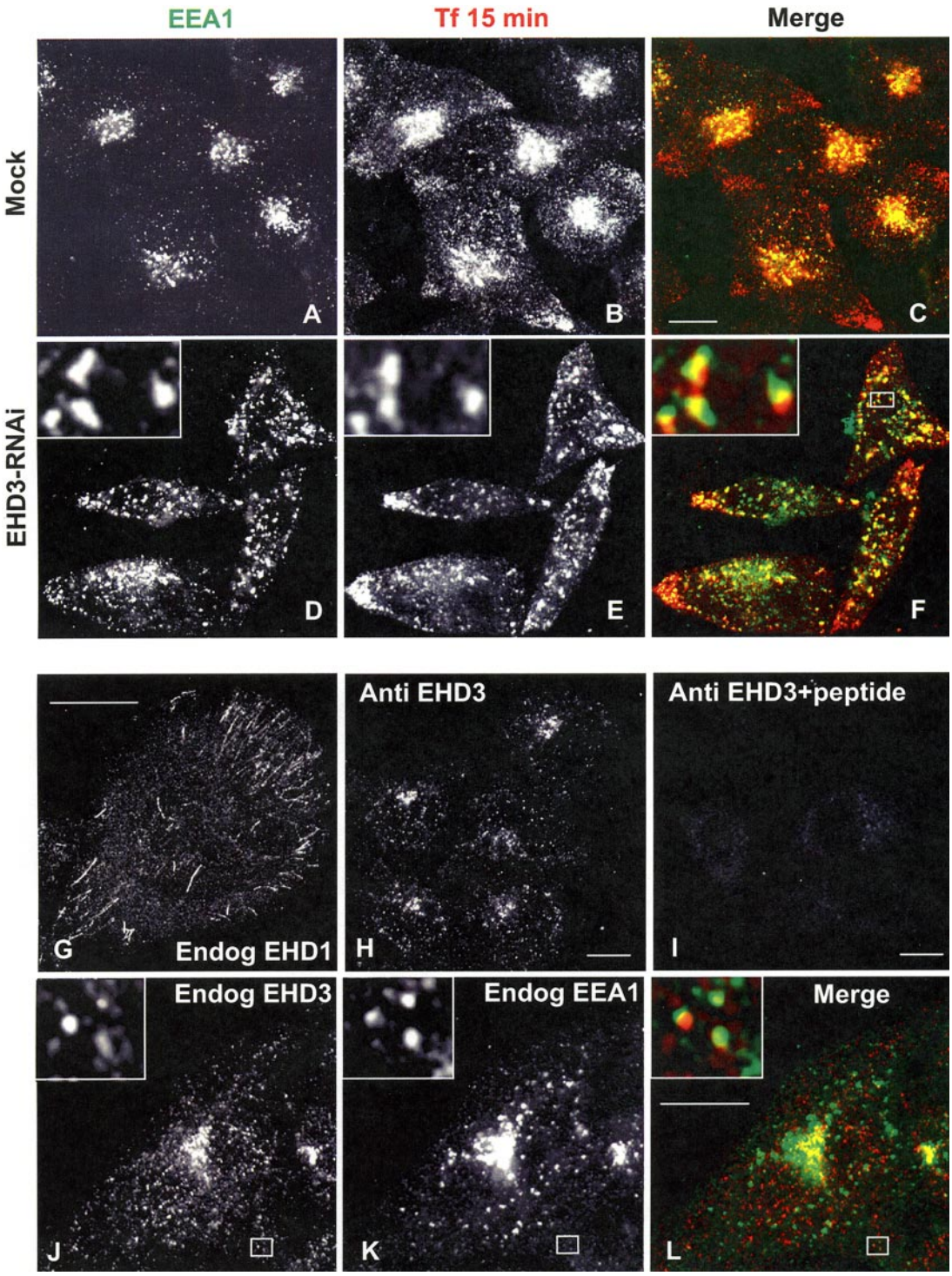

Figure 6. EHD3 is required for the normal distribution of early endosomal markers. (A–F) HeLa cells on coverglasses were Mock-treated (A–C) or treated with EHD3-RNAi (D–F). After 48 h of treatment with RNAi, all cells were subjected to a 15-min pulse with Tf-568. After fixation, cells were first incubated with monoclonal antibodies directed against endogenous EEA1 (A–F). Cells were then washed and incubated with a secondary 488-conjugated goat anti-mouse antibody before mounting on cover-slides. (G) Untransfected HeLa cells were fixed and incubated with affinity-purified polyclonal rabbit anti-EHD1 antibodies and then detected using 568-conjugated anti-rabbit antibodies. (H and I) Untransfected HeLa cells were fixed and incubated with affinity-purified polyclonal rabbit anti-EHD3 antibodies (H) or with the same antibody in the presence of 1 μM immunizing peptide (I). 568-Conjugated anti-rabbit antibodies were used for detection of EHD3. (J–L) Fixed HeLa cells were coincubated with affinity-purified polyclonal rabbit anti-EHD3 antibodies (J) and mouse monoclonal antibodies directed at EEA1 (K) by using the appropriate 568-conjugated anti-rabbit and 488-conjugated anti-mouse antibodies. The merged image is shown (L). Insets (D–F and J–L) depict enlarged regions of the cells and show partial colocalization. All images were obtained using a Zeiss LSM 5 Pascal confocal microscope. Bars (A–F, G–I, and J–L), 10 μm.

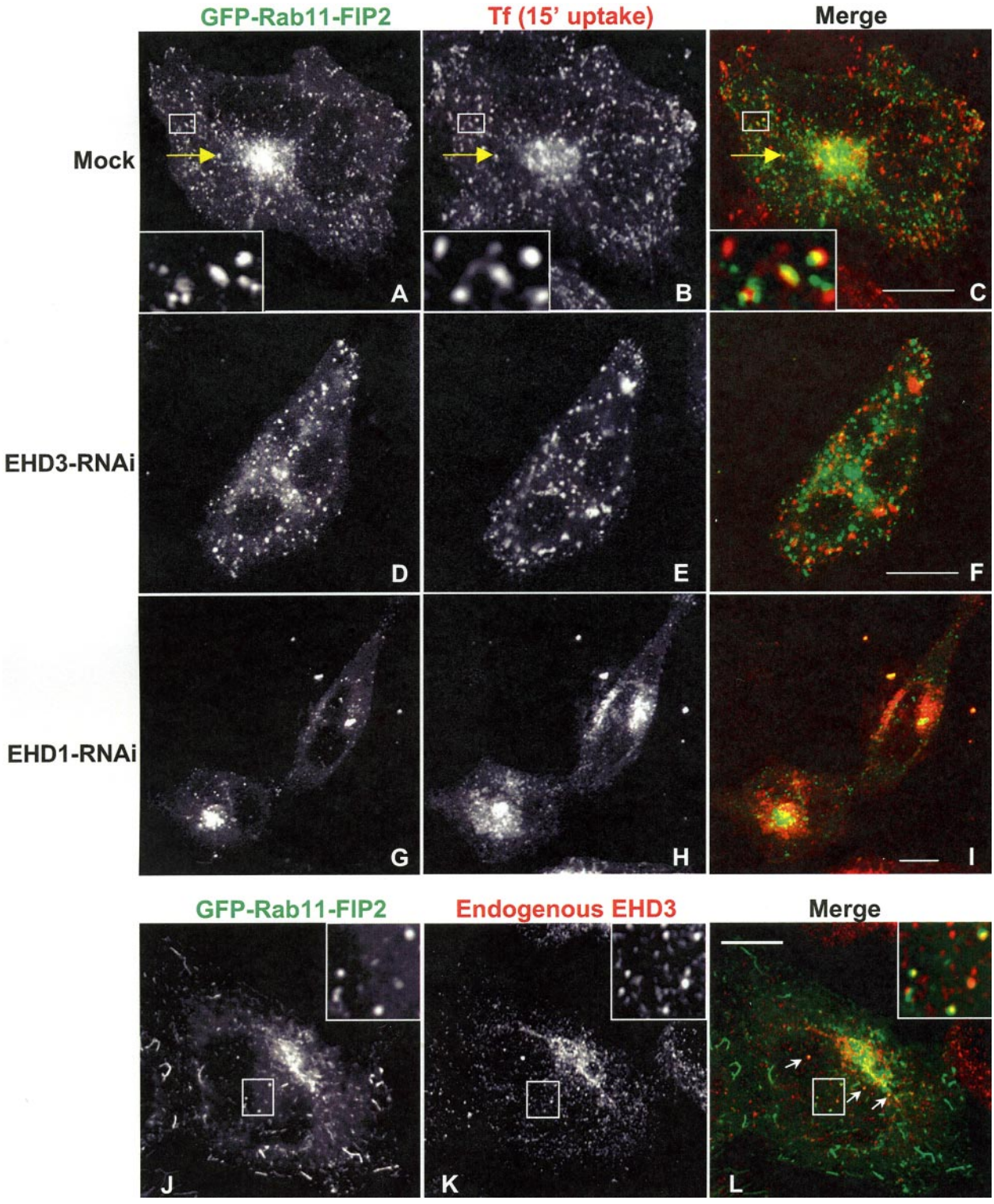

Figure 7. Loss of EHD3 impairs recruitment of Rab11-FIP2 to the perinuclear endocytic recycling compartment. (A–I) HeLa cells were Mock-treated (A–C), treated with EHD3-RNAi (D–F), or EHD1-RNAi (G–I). Cells were transiently transfected on coverglasses with GFP-Rab11-FIP2 (A–I). After 48-h treatment with RNAi, all cells were subjected to a 15-min pulse with Tf-568. After fixation, cells were mounted directly on coverslides for analysis. All images were obtained using a Zeiss LSM 5 Pascal confocal microscope. (J–L) HeLa cells were transfected on coverglasses with GFP-Rab11-FIP2 and fixed/permeabilized after 24 h. The cells were then incubated with affinity-purified rabbit polyclonal anti-EHD3 antibodies, and EHD3 was detected with 568-conjugated donkey anti-rabbit secondary antibodies. Inset and arrows depict vesicles positive for GFP-Rab11-FIP2 and endogenous EHD3. Bars, 10 μm.

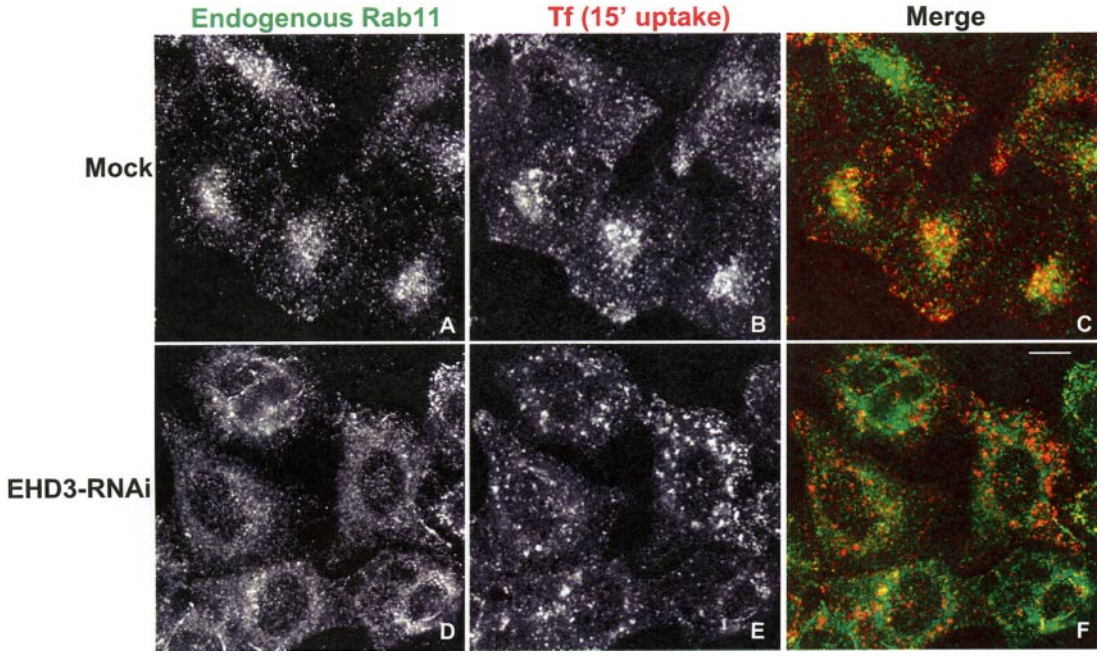

Figure 8. Loss of EHD3 affects the distribution of endogenous Rab11. (A–F) HeLa cells on coverglasses were Mock-treated (A–C) or treated with EHD3-RNAi (D–F) for 48 h and then subjected to a 15-min continuous pulse of Tf-568. The cells were then fixed in 4% paraformaldehyde and incubated with rabbit polyclonal antibody directed against endogenous Rab11. A secondary goat anti-rabbit (488 nm) antibody was used to detect Rab11 (A and D). The internalized transferrin is depicted in Mock-treated cells (B) and in EHD3-RNAi-treated cells (E). Bar, 10 μm.

directly to Rab11 by one or more of these effectors. Of the known effectors, Rab11-FIP2 stood out as an excellent candidate; it interacts with Rab11 (in both GTP- and GDP-bound forms) and myosin Vb and regulates recycling events (Hales *et al*., 2001, 2002; Cullis *et al*., 2002; Lindsay and McCaffrey, 2002). In addition, Rab11-FIP2 is the only known Rab11 effector that contains (three) NPF motifs (Cullis *et al*., 2002).

Our data support an interaction between the EHD proteins and Rab11-FIP2. When the EH domains of EHD3 and EHD1 were perturbed by the introduction of a point mutation in a conserved tryptophan residue critical for binding of the NPF motif (conserved in 95% of EH domains; de Beer *et al*., 1998, 2000; Santolini *et al*., 1999; Miliaras and Wendland, 2004; Naslavsky *et al*., 2004a), interactions with Rab11-FIP2 were abrogated. Our mapping studies have demonstrated that the second Rab11-FIP2 NPF motif is critical for binding to EHD proteins. These results are in accord with recent findings showing that Rab11-FIP2 binding to Reps1 is also mediated primarily through the second NPF motif (Cullis *et al*., 2002). The presence of the other two NPF motifs raises the possibility that Rab11-FIP2 could be interacting with other, as of yet unidentified, EH domain-containing proteins.

Overexpression of either EHD1 or EHD3 affects recruitment of Rab11-FIP2 to tubulovesicular membranes, in accord with a role for EHD proteins in regulating the subcellular localization of Rab11-FIP2. Consistent with these findings, EHD3-RNAi partially prevented the localization of Rab11 to the perinuclear region, although the effect was more modest than the accumulation of Rab11-FIP2 observed in peripheral structures. This is likely because Rab11-FIP2 is one of a number of Rab11 effectors, and we surmise that EHD3 is likely to regulate only a subpopulation of Rab11 proteins that are bound to Rab11-FIP2 at any given time. In contrast, knockdown of EHD1 expression also affected Rab11-FIP2, but it caused a greater accumulation of this effector at the ERC.

Until now, the function of EHD3 has not been addressed. On overexpression, it colocalizes with EHD1, and the two proteins hetero-oligomerize (Galperin *et al*., 2002; Figure 4B and Supplemental Figure 5). The battery of specific anti-EHD polyclonal peptide antibodies that we have designed against unique peptide sequences has allowed us, for the first time, to determine that all four endogenous EHD proteins are simultaneously expressed in mammalian cells (Figure 4A). This finding further highlights the possibility that hetero-oligomerization may play a physiologically significant role in the mode by which EHD1 and EHD3 function in vivo, and potentially regulate the binding of EHD proteins to Rab11-FIP2.

In the course of this study, an article was published demonstrating that a region of EHD1 with high probability of forming a coiled-coil was necessary for its homo-oligomerization (Lee *et al*., 2005). By identifying a single point mutant (EHD V203P) that no longer forms homo- and hetero-oligomers (Figure 4, C and D), we were able to demonstrate that EHD oligomerization is required for the binding of EHD3 and EHD1 to Rab11-FIP2. Strikingly, EHD oligomerization is required for binding to Rab11-FIP2, but not to Rabenosyn-5. Although this inequality in binding requirements is currently not clear, we speculate that the lengthy distance (~80 amino acids apart) between the first and second Rab11-FIP2 NPF motifs (both capable of binding EHD proteins) might allow this protein to bind simultaneously to two oligomerizing EHD proteins, thereby stabilizing the interaction.

We have also demonstrated that EHD3 is capable of ATP-binding and that impaired nucleotide-binding mutants (EHD3 G65R and EHD1 G65R) behaved similarly to the oligomerization mutants (EHD3 V203P and EHD1 V203P), displaying reduced binding to Rab11-FIP2. Therefore, as-

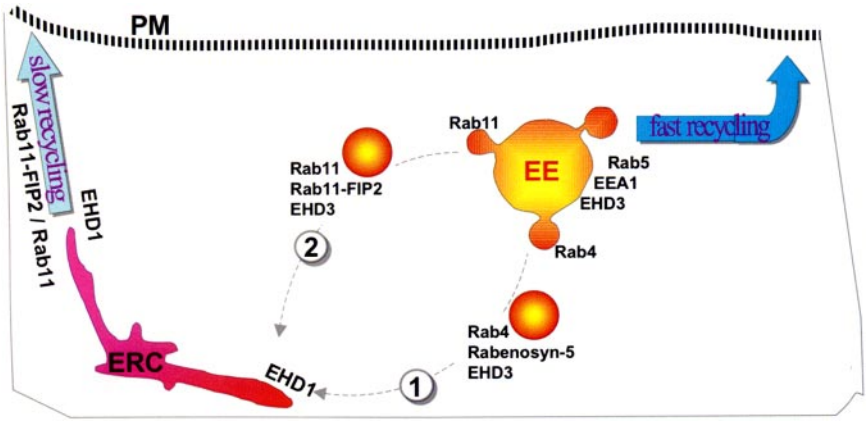

Figure 9. Model depicting the proposed roles for EHD3 in transport at the early endosome. Endogenous EHD3 is found at early endosomes and partially colocalizes with EEA1. EHD3 interacts with Rabenosyn-5 (via EH–NPF interactions), a divalent effector of Rab4/Rab5 involved both in "fast recycling" directly from the early endosome as well as in the "slower recycling" via the ERC. (1) Transient complexes comprised of EHD1/EHD3 hetero-oligomers together with Rabenosyn-5 may facilitate fusion of Rab4/Rabenosyn-5/EHD3-positive vesicles derived from the early endosome with the ERC. (2) EHD3 also binds to Rab11-FIP2 via EH–NPF interactions and may play an additional role in transport of vesicles carrying Rab11-FIP2 (and possibly Rab11) from the early endosome to the ERC, where they function in concert with EHD1 to control recycling from the ERC to the PM. EE, early endosome; ERC, endocytic recycling compartment; PM, plasma membrane.

sembly of EHD proteins in an oligomeric complex is required for optimal interaction with Rab11-FIP2. Our data therefore lead us to suggest a new role for nucleotide binding and/or oligomerization in regulating the function of the EHD EH domain, by controlling its binding with certain NPF-containing proteins such as Rab11-FIP2. Consistent with the findings of Lee *et al*. (2005), it is likely that the loss of EHD nucleotide binding impairs associations with Rab11-FIP2 as a result of the inability to form oligomers. Interestingly, both EHD1 G65R and EHD3 G65R mutants display a highly cytosolic phenotype when expressed in HeLa cells and even alter the localization of Rab11-FIP2. Although this effect could be due to residual binding of the EHD mutants to Rab11-FIP2, it is more likely that the EHD mutants sequester proteins and/or lipids that help regulate Rab11-FIP2 localization. These results further support the notion that EHD1, EHD3, and Rab11-FIP2 are involved in the regulation of a common pathway and that EHD proteins recruit Rab11-FIP2 to membrane structures.

Somewhat surprisingly, RNAi knockdown of EHD3 expression influenced trafficking events in a very different manner from that of EHD1-RNAi: there was no delivery of internalized transferrin to the ERC (Figure 5, E and H), whereas EHD1-RNAi caused internalized transferrin to accumulated at the ERC (Naslavsky *et al*., 2004a; Figure 5, D and G). Although we have measured only a modest delay in the rate of transferrin recycling upon EHD3 knockdown, recent evidence suggests that blocking transport to the ERC can actually enhance transferrin recycling, by shunting cargo to the "fast recycling" pathway (Hirst *et al*., 2005). The PI3K inhibitor LY294002 has been proposed to delay recycling through this fast recycling pathway directly from early endosomes (van Dam *et al*., 2002), and addition of this inhibitor further added to the modest delay in transferrin recycling measured with EHD3-RNAi. These data suggest a role for EHD3 at the early or sorting endosome, in regulation of cargo delivery from an early endosomal compartment to the ERC. Indeed, peripheral transferrin-containing structures induced by EHD3-RNAi are of early endosomal origin and contain classical markers for these organelles (Figure 6, D–F). Moreover, endogenous EHD3 partially colocalizes with the endogenous early endosomal marker, EEA1 (Figure 6, J–L). Thus, despite the homology exhibited between EHD1 and EHD3, they seem to regulate distinct steps along the endocytic recycling pathway and their transient hetero-oligomerization may facilitate cargo transport from one organelle to the next.

How might we attempt to incorporate these proteins into a common model for recycling en route from early endosomes to the plasma membrane? Receptors at the early endosome bound for recycling via the ERC are segregated into micromembrane domains that bud into vesicles (Sonnichsen *et al*., 2000) (see Figure 9 model). Within these domains, Rab4 might recruit effectors, such as Rabenosyn-5 (Nielsen *et al*., 2000) to the budding vesicles, where EHD3 is localized to the cytosolic face (Figure 9, pathway 1). Rab4-containing early endosomal-derived vesicles might use Rabenosyn-5 as a "connector" to EHD proteins, allowing the initiation of contact with the ERC membrane via homo- and hetero-oligomerization with EHD1 located at the ERC. The transient interaction between EHD1 and Rabenosyn-5 (Naslavsky *et al*., 2004a) might not be sufficient to mediate this transport step; it is possible that an interaction between EHD1, EHD3, and Rabenosyn-5 provides greater scaffolding for SNARE pairing and fusion of vesicles with the ERC.

In parallel, and perhaps in distinct micromembrane domains (Sonnichsen *et al*., 2000), nucleotide-loaded EHD3 located at the early endosome can homo- or hetero-oligomerize (with itself or EHD1) at early endosomes or at ERC membranes, thereby establishing a bond with Rab11 sorting/recycling machinery via Rab11-FIP2 (Figure 9, pathway 2). At the same time, it is possible that EHD1-mediated exit from the ERC also facilitates the return of "early endosome accessory proteins," such as Rab11-FIP2, back to the early endosome.

The interaction of Rab11-FIP2 with other EH domain-containing proteins localized to endosomes, such as Reps1, may further help connect early endosome to ERC transport (Cullis *et al*., 2002). Direct connections between early endosomes and the ERC may also be mediated by other Rab11 effectors, such as the Rab coupling protein, which provides a link between Rab4 and Rab11 (Lindsay *et al*., 2002; Lindsay and McCaffrey, 2004b; Peden *et al*., 2004). The identification of new proteins involved in the regulation of this pathway is important to our understanding of the mechanisms controlling endocytic recycling. This study provides the first link between EHD-family proteins and Rab11-mediated transport events and sheds new light on the mode by which Rab- and EHD-family proteins coordinately control these complex endocytic transport events.

ACKNOWLEDGMENTS

We thank Drs. M. Horowitz, C. Arighi, J. Donaldson, and especially R. C. Aguilar for the critical reading of this manuscript and helpful discussions. We are also very grateful to Dr. R. Prekeris for the generous gift of Rab11-FIP2 antibodies and constructs. This work was supported by National Institutes of Health Grant P20 RR018759 from the National Center for Research Resources and by American Heart Association Grant 0460001z.

REFERENCES

Benmerah, A. (2004). Endocytosis: signaling from endocytic membranes to the nucleus. Curr. Biol. *14*, R314–316.

Berger, B., Wilson, D. B., Wolf, E., Tonchev, T., Milla, M., and Kim, P. S. (1995). Predicting coiled coils by use of pairwise residue correlations. Proc. Natl. Acad. Sci. USA *92*, 8259–8263.

Braun, A., Agelet, R.P.I., Dahlhaus, R., Koch, D., Fonarev, P., Grant, B. D., Kessels, M. M., and Qualmann, B. (2005). EHD proteins associate with syndapin I and II and such interactions play a crucial role in endosomal recycling. Mol. Biol. Cell *16*, 3642–3658.

Caplan, S., Hartnell, L. M., Aguilar, R. C., Naslavsky, N., and Bonifacino, J. S. (2001). Human Vam6p promotes lysosome clustering and fusion in vivo. J. Cell Biol. *154*, 109–122.

Caplan, S., Naslavsky, N., Hartnell, L. M., Lodge, R., Polishchuk, R. S., Donaldson, J. G., and Bonifacino, J. S. (2002). A tubular EHD1-containing compartment involved in the recycling of major histocompatibility complex class I molecules to the plasma membrane. EMBO J. *21*, 2557–2567.

Conner, S. D., and Schmid, S. L. (2003). Regulated portals of entry into the cell. Nature *422*, 37–44.

Cullis, D. N., Philip, B., Baleja, J. D., and Feig, L. A. (2002). Rab11-FIP2, an adaptor protein connecting cellular components involved in internalization and recycling of epidermal growth factor receptors. J. Biol. Chem. *277*, 49158–49166.

Daro, E., van der Sluijs, P., Galli, T., and Mellman, I. (1996). Rab4 and cellubrevin define different early endosome populations on the pathway of transferrin receptor recycling. Proc. Natl. Acad. Sci. USA *93*, 9559–9564.

de Beer, T., Carter, R. E., Lobel-Rice, K. E., Sorkin, A., and Overduin, M. (1998). Structure and Asn-Pro-Phe binding pocket of the Eps15 homology domain. Science *281*, 1357–1360.

de Beer, T., Hoofnagle, A. N., Enmon, J. L., Bowers, R. C., Yamabhai, M., Kay, B. K., and Overduin, M. (2000). Molecular mechanism of NPF recognition by EH domains. Nat. Struct. Biol. *7*, 1018–1022.

Elbashir, S. M., Harborth, J., Lendeckel, W., Yalcin, A., Weber, K., and Tuschl, T. (2001). Duplexes of 21-nucleotide RNAs mediate RNA interference in cultured mammalian cells. Nature *411*, 494–498.

Fan, G. H., Lapierre, L. A., Goldenring, J. R., Sai, J., and Richmond, A. (2004). Rab11-family interacting protein 2 and myosin Vb are required for CXCR2 recycling and receptor-mediated chemotaxis. Mol. Biol. Cell *101*, 2115–2124.

Galperin, E., Benjamin, S., Rapaport, D., Rotem-Yehudar, R., Tolchinsky, S., and Horowitz, M. (2002). EHD3: a protein that resides in recycling tubular and vesicular membrane structures and interacts with EHD1. Traffic *3*, 575–589.

Grant, B., Zhang, Y., Paupard, M. C., Lin, S. X., Hall, D. H., and Hirsh, D. (2001). Evidence that RME-1, a conserved *C. elegans* EH-domain protein, functions in endocytic recycling. Nat. Cell Biol. *3*, 573–579.

Gruenberg, J., and Maxfield, F. R. (1995). Membrane transport in the endocytic pathway. Curr. Opin. Cell Biol. *7*, 552–563.

Guilherme, A., Soriano, N. A., Bose, S., Holik, J., Bose, A., Pomerleau, D. P., Furcinitti, P., Leszyk, J., Corvera, S., and Czech, M. P. (2004a). EHD2 and the novel EH domain binding protein EHBP1 couple endocytosis to the actin cytoskeleton. J. Biol. Chem. *279*, 10593–10605.

Guilherme, A., Soriano, N. A., Furcinitti, P. S., and Czech, M. P. (2004b). Role of EHD1 and EHBP1 in perinuclear sorting and insulin-regulated GLUT4 recycling in 3T3–L1 adipocytes. J. Biol. Chem. *279*, 40062–40075.

Hales, C. M., Griner, R., Hobdy-Henderson, K. C., Dorn, M. C., Hardy, D., Kumar, R., Navarre, J., Chan, E. K., Lapierre, L. A., and Goldenring, J. R. (2001). Identification and characterization of a family of Rab11-interacting proteins. J. Biol. Chem. *276*, 39067–39075.

Hales, C. M., Vaerman, J. P., and Goldenring, J. R. (2002). Rab11 family interacting protein 2 associates with Myosin Vb and regulates plasma membrane recycling. J. Biol. Chem. *277*, 50415–50421.

Hao, M., and Maxfield, F. R. (2000). Characterization of rapid membrane internalization and recycling. J. Biol. Chem. *275*, 15279–15286.

Hirst, J., Borner, G. H., Harbour, M., and Robinson, M. S. (2005). The aftiphilin/p200/gamma-synergin complex. Mol. Biol. Cell *16*, 2554–2565.

Hopkins, C. R., and Trowbridge, I. S. (1983). Internalization and processing of transferrin and the transferrin receptor in human carcinoma A431 cells. J. Cell Biol. *97*, 508–521.

Jacobson, G. R., and Rosenbusch, J. P. (1976). ATP binding to a protease-resistant core of actin. Proc. Natl. Acad. Sci. USA *73*, 2742–2746.

Kinosian, H. J., Selden, L. A., Estes, J. E., and Gershman, L. C. (1993). Nucleotide binding to actin. Cation dependence of nucleotide dissociation and exchange rates. J. Biol. Chem. *268*, 8683–8691.

Lapierre, L. A., Dorn, M. C., Zimmerman, C. F., Navarre, J., Burnette, J. O., and Goldenring, J. R. (2003). Rab11b resides in a vesicular compartment distinct from Rab11a in parietal cells and other epithelial cells. Exp. Cell Res. *290*, 322–331.

Lee, D. W., Zhao, X., Scarselletta, S., Schweinsberg, P. J., Eisenberg, E., Grant, B. D., and Greene, L. E. (2005). ATP Binding regulates oligomerization and endosome association of RME-1 family proteins. J. Biol. Chem. *280*, 17213–17220.

Lin, S. X., Grant, B., Hirsh, D., and Maxfield, F. R. (2001). Rme-1 regulates the distribution and function of the endocytic recycling compartment in mammalian cells. Nat. Cell Biol. *3*, 567–572.

Lindsay, A. J., Hendrick, A. G., Cantalupo, G., Senic-Matuglia, F., Goud, B., Bucci, C., and McCaffrey, M. W. (2002). Rab coupling protein (RCP), a novel Rab4 and Rab11 effector protein. J. Biol. Chem. *277*, 12190–12199.

Lindsay, A. J., and McCaffrey, M. W. (2002). Rab11-FIP2 functions in transferrin recycling and associates with endosomal membranes via its COOH-terminal domain. J. Biol. Chem. *277*, 27193–27199.

Lindsay, A. J., and McCaffrey, M. W. (2004a). The C2 domains of the class I Rab11 family of interacting proteins target recycling vesicles to the plasma membrane. J. Cell Sci. *117*, 4365–4375.

Lindsay, A. J., and McCaffrey, M. W. (2004b). Characterisation of the Rab binding properties of Rab coupling protein (RCP) by site-directed mutagenesis. FEBS Lett. *571*, 86–92.

Maxfield, F. R., and McGraw, T. E. (2004). Endocytic recycling. Nat. Rev. Mol. Cell. Biol. *5*, 121–132.

Mellman, I. (1996). Endocytosis and molecular sorting. Annu. Rev. Cell Dev. Biol. *12*, 575–625.

Miliaras, N. B., and Wendland, B. (2004). EH proteins: multivalent regulators of endocytosis (and other pathways). Cell Biochem. Biophys. *41*, 295–318.

Mintz, L., Galperin, E., Pasmanik-Chor, M., Tulzinsky, S., Bromberg, Y., Kozak, C. A., Joyner, A., Fein, A., and Horowitz, M. (1999). EHD1–an EH-domain-containing protein with a specific expression pattern. Genomics *59*, 66–76.

Naslavsky, N., Boehm, M., Backlund, P. S., Jr., and Caplan, S. (2004a). Rabenosyn-5 and EHD1 interact and sequentially regulate protein recycling to the plasma membrane. Mol. Biol. Cell *15*, 2410–2422.

Naslavsky, N., and Caplan, S. (2005). C-terminal EH-domain containing proteins: consensus for a role in endocytic trafficking, EH? J. Cell Sci. *118*, 4093–4101.

Naslavsky, N., Weigert, R., and Donaldson, J. G. (2004b). Characterization of a non-clathrin endocytic pathway: membrane cargo and lipid requirements. Mol. Biol. Cell *15*, 3542–3552.

Nichols, B. J., and Lippincott-Schwartz, J. (2001). Endocytosis without clathrin coats. Trends Cell Biol. *11*, 406–412.

Nielsen, E., Christoforidis, S., Uttenweiler-Joseph, S., Miaczynska, M., Dewitte, F., Wilm, M., Hoflack, B., and Zerial, M. (2000). Rabenosyn-5, a novel Rab5 effector, is complexed with hVPS45 and recruited to endosomes through a FYVE finger domain. J. Cell Biol. *151*, 601–612.

Park, M., Penick, E. C., Edwards, J. G., Kauer, J. A., and Ehlers, M. D. (2004a). Recycling endosomes supply AMPA receptors for LTP. Science *305*, 1972–1975.

Park, S. Y., Ha, B. G., Choi, G. H., Ryu, J., Kim, B., Jung, C. Y., and Lee, W. (2004b). EHD2 interacts with the insulin-responsive glucose transporter (GLUT4) in rat adipocytes and may participate in insulin-induced GLUT4 recruitment. Biochemistry *43*, 7552–7562.

Peden, A. A., Schonteich, E., Chun, J., Junutula, J. R., Scheller, R. H., and Prekeris, R. (2004). The RCP-Rab11 complex regulates endocytic protein sorting. Mol. Biol. Cell *15*, 3530–3541.

Picciano, J. A., Ameen, N., Grant, B. D., and Bradbury, N. A. (2003). Rme-1 regulates the recycling of the cystic fibrosis transmembrane conductance regulator. Am. J. Physiol. *285*, C1009–C1018.

Polo, S., Confalonieri, S., Salcini, A. E., and Di Fiore, P. P. (2003). EH and UIM: endocytosis and more. Sci. STKE *2003*, re17.

Prekeris, R. (2003). Rabs, Rips, FIPs, and endocytic membrane traffic. Scientific World Journal *3*, 870–880.

Prekeris, R., Davies, J. M., and Scheller, R. H. (2001). Identification of a novel Rab11/25 binding domain present in Eferin and Rip proteins. J. Biol. Chem. *276*, 38966–38970.

Ren, M., Xu, G., Zeng, J., De Lemos-Chiarandini, C., Adesnik, M., and Sabatini, D. D. (1998). Hydrolysis of GTP on rab11 is required for the direct delivery of transferrin from the pericentriolar recycling compartment to the cell surface but not from sorting endosomes. Proc. Natl. Acad. Sci. USA *95*, 6187–6192.

Rotem-Yehudar, R., Galperin, E., and Horowitz, M. (2001). Association of insulin-like growth factor 1 receptor with EHD1 and SNAP29. J. Biol. Chem. *276*, 33054–33060.

Saitou, N., and Nei, M. (1987). The neighbor-joining method: a new method for reconstructing phylogenetic trees. Mol. Biol. Evol. *4*, 406–425.

Salcini, A. E., Confalonieri, S., Doria, M., Santolini, E., Tassi, E., Minenkova, O., Cesareni, G., Pelicci, P. G., and Di Fiore, P. P. (1997). Binding specificity and in vivo targets of the EH domain, a novel protein-protein interaction module. Genes Dev. *11*, 2239–2249.

Santolini, E., Salcini, A. E., Kay, B. K., Yamabhai, M., and Di Fiore, P. P. (1999). The EH network. Exp. Cell Res. *253*, 186–209.

Shao, Y., Akmentin, W., Toledo-Aral, J. J., Rosenbaum, J., Valdez, G., Cabot, J. B., Hilbush, B. S., and Halegoua, S. (2002). Pincher, a pinocytic chaperone for nerve growth factor/TrkA signaling endosomes. J. Cell Biol. *157*, 679–691.

Sheff, D., Pelletier, L., O'Connell, C. B., Warren, G., and Mellman, I. (2002). Transferrin receptor recycling in the absence of perinuclear recycling endosomes. J. Cell Biol. *156*, 797–804.

Sheff, D. R., Daro, E. A., Hull, M., and Mellman, I. (1999). The receptor recycling pathway contains two distinct populations of early endosomes with different sorting functions. J. Cell Biol. *145*, 123–139.

Smith, C. A., Dho, S. E., Donaldson, J., Tepass, U., and McGlade, C. J. (2004). The cell fate determinant Numb interacts with EHD/Rme-1 family proteins and has a role in endocytic recycling. Mol. Biol. Cell *15*, 3698–3708.

Sonnichsen, B., De Renzis, S., Nielsen, E., Rietdorf, J., and Zerial, M. (2000). Distinct membrane domains on endosomes in the recycling pathway visualized by multicolor imaging of Rab4, Rab5, and Rab11. J. Cell Biol. *149*, 901–914.

Ullrich, O., Reinsch, S., Urbe, S., Zerial, M., and Parton, R. G. (1996). Rab11 regulates recycling through the pericentriolar recycling endosome. J. Cell Biol. *135*, 913–924.

van Dam, E. M., Ten Broeke, T., Jansen, K., Spijkers, P., and Stoorvogel, W. (2002). Endocytosed transferrin receptors recycle via distinct dynamin and phosphatidylinositol 3-kinase-dependent pathways. J. Biol. Chem. *277*, 48876–48883.

van der Sluijs, P., Hull, M., Webster, P., Male, P., Goud, B., and Mellman, I. (1992). The small GTP-binding protein rab4 controls an early sorting event on the endocytic pathway. Cell *70*, 729–740.

Xu, Y., Shi, H., Wei, S., Wong, S. H., and Hong, W. (2004). Mutually exclusive interactions of EHD1 with GS32 and Syndapin II. Mol. Membr. Biol. *21*, 269–277.

Yamashiro, D. J., Tycko, B., Fluss, S. R., and Maxfield, F. R. (1984). Segregation of transferrin to a mildly acidic (pH 6.5) para-Golgi compartment in the recycling pathway. Cell *37*, 789–800.

Zeng, J., *et al.* (1999). Identification of a putative effector protein for rab11 that participates in transferrin recycling. Proc. Natl. Acad. Sci. USA *96*, 2840–2845.